Pleckstrin homology domain-interacting protein (PHIP) as a marker and mediator of melanoma metastasis

David De Semir[a,1], Mehdi Nosrati[a,1], Vladimir Bezrookove[a,1], Altaf A. Dar[a,1], Scot Federman[a], Geraldine Bienvenu[a], Suraj Venna[a,2], Javier Rangel[a], Joan Climent[b,3], Tanja M. Meyer Tamgüney[b], Suresh Thummala[a,1], Schuyler Tong[c], Stanley P. L. Leong[d,1], Chris Haqq[e], Paul Billings[f,g], James R. Miller III[a,1], Richard W. Sagebiel[a,1], Robert Debs[c], and Mohammed Kashani-Sabet[a,1,4]

[a]Auerback Melanoma Research Laboratory and Melanoma Center, [b]Helen Diller Family Comprehensive Cancer Center, and Departments of [d]Surgery and [e]Urology, University of California, San Francisco, CA 94115; [c]California Pacific Medical Center Research Institute, San Francisco, CA 94107; [f]Life Technologies, Inc., Carlsbad, CA 92008; and [g]Melanoma Diagnostics, Inc., Fremont, CA 94536

Edited* by James E. Cleaver, University of California, San Francisco, CA, and approved March 27, 2012 (received for review December 9, 2011)

Although melanomas with mutant v-Raf murine sarcoma viral oncogene homolog B1 (BRAF) can now be effectively targeted, there is no molecular target for most melanomas expressing wild-type BRAF. Here, we show that the activation of Pleckstrin homology domain-interacting protein (PHIP), promotes melanoma metastasis, can be used to classify a subset of primary melanomas, and is a prognostic biomarker for melanoma. Systemic, plasmid-based shRNA targeting of Phip inhibited the metastatic progression of melanoma, whereas stable suppression of Phip in melanoma cell lines suppressed metastatic potential and prolonged the survival of tumor-bearing mice. The human *PHIP* gene resides on 6q14.1, and although 6q loss has been observed in melanoma, the *PHIP* locus was preserved in melanoma cell lines and patient samples, and its overexpression was an independent adverse predictor of survival in melanoma patients. In addition, a high proportion of PHIP-overexpressing melanomas harbored increased *PHIP* copy number. PHIP-overexpressing melanomas include tumors with wild-type BRAF, neuroblastoma RAS viral (v-ras) oncogene homolog, and phosphatase and tensin homolog, demonstrating PHIP activation in triple-negative melanoma. These results describe previously unreported roles for PHIP in predicting and promoting melanoma metastasis, and in the molecular classification of melanoma.

The successful development of targeted therapy for melanomas harboring *BRAF* mutations has garnered significant attention, given the promising results of small molecule inhibitors of mutant BRAF (1). However, the molecular basis underlying the metastasis of the ≈50% of all human melanomas that lack a *BRAF* mutation, and specific targets for the therapy of these melanomas, is unclear. As a result, "triple-negative melanoma" patients, whose tumors harbor wild-type *v-Raf murine sarcoma viral oncogene homolog B1* (*BRAF*), *neuroblastoma RAS viral (v-ras) oncogene homolog* (*NRAS*), and phosphatase and tensin homolog (*PTEN*) (the most common mutations observed in melanoma), are not candidates for most targeted therapies developed to date.

The type I insulin-like growth factor receptor (IGF1R) signaling pathway has been recognized to play an increasingly important role in tumorigenesis (2, 3). Binding of IGF1 or IGF2 to IGF1R results in phosphorylation of tyrosine and carboxyl-terminal serine residues that form binding sites for the insulin-receptor substrate (IRS) docking proteins. IRS activation results in PI3K recruitment and AKT activation (4). Efficient docking of IRS proteins is mediated via their pleckstrin homology domain. Pleckstrin homology domain-interacting protein (PHIP), initially identified through interactions with the pleckstrin homology domain of IRS proteins, has been shown to mediate transcriptional responses in pancreatic islet cells (5), and is important for postnatal growth (6). Previously, we identified *PHIP* as the gene most highly overexpressed in metastatic melanomas, compared with primary tumors by cDNA microarray analysis (7). Although PHIP plays a role in IGF signaling, its involvement in cancer has not been reported.

Results

To assess the potential role of PHIP in melanoma progression, we examined the anti-tumor activity produced by shRNAs targeting different regions of murine *Phip* mRNA. Systemic, cationic liposome:DNA complex (CLDC)-mediated delivery of these constructs identified shRNA723 as the most effective shRNA (Fig. S1*A*). Transient transfection of siRNA723 oligonucleotides resulted in 80% reduction in *Phip* expression by quantitative RT-PCR (qRT-PCR) (Fig. 1*A*). Transient transfection of a plasmid encoding shRNA723 into B16-F10 melanoma cells significantly reduced their invasion into matrigel, compared with both vector control and a control shRNA targeting firefly luciferase (luc) ($P < 0.05$; Fig. 1*B*). Furthermore, two intravenous, CLDC-based injections of shRNA723 into C57BL/6 mice bearing metastatic B16-F10 melanoma significantly reduced metastatic tumor counts compared with the anti-luc shRNA control ($P < 0.05$; Fig. 1*C*).

We then developed B16-F10 transformants stably expressing shRNA723. Pooled shRNA-expressing B16-F10 clones exhibited significantly reduced *Phip* expression (Fig. 2 *A* and *B*) compared with pooled control clones expressing anti-luc shRNA. B16-F10 clones expressing shRNA723 exhibited significantly reduced invasion into matrigel ($P < 0.05$; Fig. 2*C*), and i.v. inoculation of shRNA723-expressing B16-F10 cells significantly prolonged the survival of tumor-bearing C57BL/6 mice compared with anti-luc shRNA-expressing clones ($P < 0.001$; Fig. 2*D*). These studies demonstrate a direct relationship between the level of *Phip* expression and the metastatic potential of melanoma. Similar inhibition of *Phip* expression, and reduction of the invasion and metastasis of B16-F10 melanoma, were demonstrated when shRNA723-expressing cells were compared with B16-F10 cells

Author contributions: D.D.S., V.B., and M.K.-S. designed research; D.D.S., M.N., V.B., A.A.D., G.B., S.V., J.R., J.C., T.M.M.T., S. Thummala, S. Tong, and R.W.S. performed research; S.V., J.C., T.M.M.T., S. Thummala, S.P.L.L., J.R.M., and R.D. contributed new reagents/analytic tools; D.D.S., M.N., V.B., A.A.D., S.F., J.R., J.C., S. Tong, S.P.L.L., C.H., P.B., J.R.M., R.W.S., R.D., and M.K.-S. analyzed data; and D.D.S., V.B., T.M.M.T., C.H., P.B., J.R.M., R.W.S., R.D., and M.K.-S. wrote the paper.

Conflict of interest statement: M.K.-S. and P.B. own stock in Melanoma Diagnostics, Inc.

*This Direct Submission article had a prearranged editor.

Freely available online through the PNAS open access option.

[1]Present address: Center for Melanoma Research and Treatment, California Pacific Medical Center and California Pacific Medical Center Research Institute, San Francisco, CA 94107.

[2]Present address: Washington Cancer Institute, Washington, DC 20010.

[3]Present address: Instituto de Investigacion Sanitaria INCLIVA, 46010 Valencia, Spain.

[4]To whom correspondence should be addressed. E-mail: kashani@cpmcri.org.

This article contains supporting information online at www.pnas.org/lookup/suppl/doi:10.1073/pnas.1119949109/-/DCSupplemental.

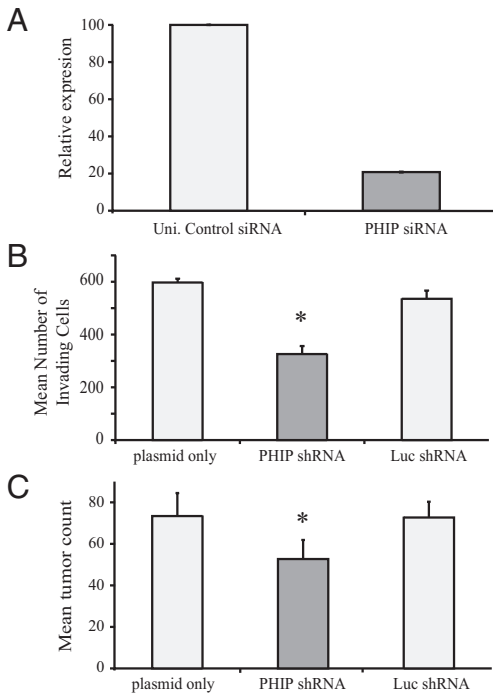

Fig. 1. Effects of CLDC-mediated expression of anti-*Phip* shRNA in murine models. (*A*) Expression of *Phip* by qRT-PCR in B16-F10 cells transfected with oligonucleotides encoding anti-*Phip* siRNA or a universal siRNA control sequence. (*B*) Invasive capacity of B16-F10 cells treated with CLDC expressing anti-*Phip* shRNA compared with vector alone or vector encoding anti-luc shRNA. (*C*) Quantification of total tumor counts in the lungs of B16-F10-bearing C57BL/6 mice i.v. injected with CLDC encoding anti-*Phip* shRNA compared with vector alone or vector encoding anti-luc shRNA. *$P < 0.05$ versus either control.

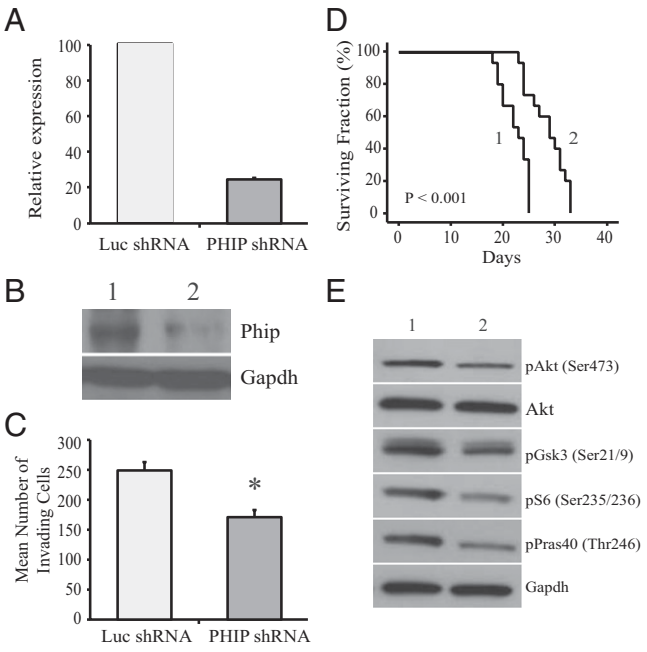

Fig. 2. Effects of stable expression of anti-*Phip* shRNA. (*A*) Expression of *Phip* by qRT-PCR in B16-F10 cells stably transfected with anti-*Phip* shRNA compared with vector encoding anti-luc shRNA. (*B*) Western blot analysis of Phip and Gapdh in B16-F10 stable transformants expressing anti-luc shRNA (lane 1) or anti-*Phip* shRNA (lane 2). Phip levels were reduced by 70% in anti-*Phip* shRNA-expressing cells. (*C*) Invasive capacity of B16-F10 cells stably transfected with anti-*Phip* shRNA was reduced by 45% compared with controls expressing anti-luc shRNA. (*D*) Kaplan–Meier analysis of survival of C57BL/6 mice i.v. injected with B16-F10 cells stably expressing anti-luc shRNA (curve 1) or anti-*Phip* shRNA (curve 2), with a >25% prolongation of median survival in the anti-*Phip* shRNA group. (*E*) Western blot analysis of pAkt and proteins downstream of Akt after stable suppression of *Phip* (lane 1, control; lane 2, anti-*Phip* shRNA). *$P < 0.05$ versus control.

stably expressing a mutant, inactivated shRNA723 (mshRNA723) (Fig. S1 *B–D*).

Given the important role of Akt in the IGF axis (4), we then assessed whether Phip was involved in Akt activation. shRNA723-expressing clones showed reduced levels of phosphorylated Akt (Ser473), with no difference in total Akt levels (Fig. 2*E*). This down-regulation was accompanied by decreased phosphorylation of three proteins downstream of Akt (Gsk3, S6, and Pras40; Fig. 2*E*).

Because of the uncharacterized role of PHIP in cancer, we performed cDNA microarray analysis to identify the global patterns of gene expression after suppression of *Phip* expression. Significance analysis of microarrays identified 51 down-regulated genes (including *Igf2* and *Tln1)* and 184 overexpressed genes (including *Phf17)* in shRNA723-expressing cells (Fig. 3 *A* and *B*). The differential expression of these three genes was confirmed by qRT-PCR (Fig. 3*C*). Thus, PHIP can regulate the expression of upstream mediators of the IGF axis and downstream mediators of tumor cell invasion (8).

Having demonstrated Phip's functional role in promoting murine melanoma metastasis, we examined its impact on human melanoma progression. We performed immunohistochemical analysis of PHIP expression on a tissue microarray cohort of 345 patients with primary cutaneous melanoma (9) and scored the specimens for intensity of PHIP immunostaining on a 0–3 scale (Fig. S2 *A–D*). High levels of PHIP expression were found in each histological subtype of melanoma and accounted for almost one-third of the melanomas in this cohort (112/345, or 32.5%). High PHIP expression correlated significantly with the presence of ulceration ($P = 0.005$, logistic regression), an adverse prognostic factor incorporated into the staging classification for melanoma (10) whose biologic basis is poorly understood. By Kaplan–Meier analysis, PHIP overexpression was significantly predictive of reduced distant metastasis-free survival (DMFS, $P = 0.01$; Fig. S2*E*) and disease-specific survival (DSS, $P = 0.002$, Fig. 4*A*). By multivariate Cox regression analysis, PHIP overexpression was an independent predictor of DMFS (Table S1) and DSS (Table S2). Thus, PHIP overexpression directly correlated with the progression of distant metastases, and with reduced survival, in both murine and human melanoma.

The human *PHIP* gene resides on the 6q14.1 locus. Deletions of the 6q arm have been shown in melanoma (11) and have been suggested as a possible diagnostic marker (12). Therefore, we assessed *PHIP* copy number, in combination with probes representing the centromere of chromosome 6, using interphase fluorescence in situ hybridization (FISH) in 78 primary melanomas from the TMA cohort on which PHIP immunohistochemical scores were available (Fig. 4 *B* and *C* and Table S3). FISH analysis revealed that the *PHIP* locus was still present in all 78 melanomas examined. Importantly, there was a significant correlation between *PHIP* copy number (assessed as a percentage of cells with three or more copies) and the corresponding PHIP immunohistochemical scores (Fig. 4*C*; $P < 0.001$). Melanomas with immunohistochemical scores of 1–3 had a significantly higher percentage of cells with increased copy number compared with melanomas with a PHIP score of 0 ($P < 0.002$). In addition, 80.6% of PHIP 3 melanomas had three or more copies of the *PHIP* locus. Although we found no evidence of amplification, because *PHIP* copy number remains comparable with chromosome 6 centromeric copy number (Table S3), increased copy number of the *PHIP*

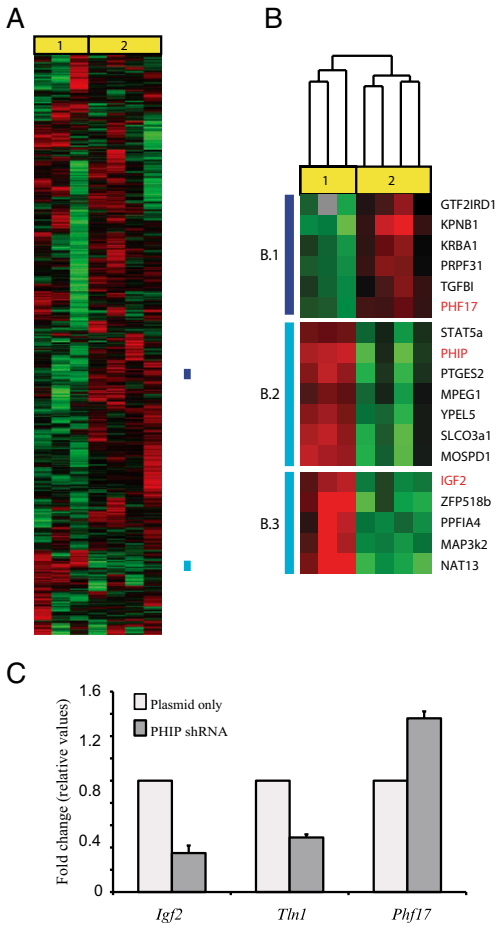

Fig. 3. Identification of genes in the *Phip* signal transduction pathway. (*A*) Gene expression profiles using supervised hierarchical analysis of triplicate clones of B16-F10 cells stably transfected with control vector (1) or anti-*Phip* shRNA (2). (*B*) SAM analysis of differentially expressed genes after stable shRNA-mediated suppression of *Phip* in B16-F10 cells. Nodes of gene expression selected demonstrating differential expression of *Phip*, *Phf17*, and *Igf2*. (*C*) Quantitative RT-PCR of *Igf2, Tln1*, and *Phf17* expression in B16-F10 stable transformants expressing control vector or anti-*Phip* shRNA as normalized to levels of Histone gene expression.

locus (and its significant correlation with immunopositivity for the PHIP protein) further supports its role as a melanoma progression gene.

Next, based on PHIP's activation of AKT, we characterized which molecular subtypes of melanomas overexpress PHIP. AKT activation in melanoma is thought to occur primarily because of either *NRAS* mutation or *BRAF* mutation coupled with *PTEN* loss (13, 14). We hypothesized that if PHIP overexpression is sufficient for AKT activation, then PHIP-overexpressing tumors may not commonly harbor other mutations known to activate AKT. We analyzed 39 primary and metastatic melanomas with high levels of PHIP expression for *NRAS* and *BRAF* mutations, and for *PTEN* allelic copy number. Fifty-six percent of the cases analyzed harbored wild-type *NRAS*, *BRAF*, and *PTEN*, whereas 26% harbored either mutant *BRAF* or *PTEN*. Only 18% were found to harbor either *NRAS* mutation or *BRAF* mutation together with *PTEN* copy number loss. Thus, PHIP-overexpressing melanomas were predominately characterized either by a triple-negative genotype or by mutant BRAF with wild-type *NRAS* and *PTEN*. Recently, β-catenin mutations have been shown to promote the progression of melanomas harboring BRAF and PTEN mutations (15). We therefore analyzed 10 high PHIP-expressing triple-negative melanomas for β-catenin mutations at six different sites (previously described in melanoma; COSMIC database) and found no mutations at any of these sites. These results show that PHIP levels can be activated in a unique molecular subset of melanoma independent of mutations in these other four genes.

We then assessed PHIP levels in a panel of human melanoma cell lines. The C8161.9 and LOX cell lines expressed higher levels of PHIP compared with D05 and 1205Lu cells (Fig. 4*D*). FISH analysis of the *PHIP* locus (along with probes representing the centromere of chromosome 6) revealed again not only that this gene is not lost, but that C8161.9 and LOX cells had increased copies of *PHIP*, compared with the two low-expressing cell lines (Fig. 4*E*). C8161.9 cells were selected for further analysis, because they exhibit a triple-negative genotype. Stable expression of an anti-human *PHIP* shRNA127738 (distinct from shRNA723) reduced PHIP protein levels (Fig. 5 *A* and *B* and Fig. S3*A*), with consequently reduced TLN1 (Fig. 5*A* and Fig. S3*B*) and phosphorylated AKT levels (Fig. 5*C*), and suppressed invasive (Fig. 5*D*) and metastatic potential (Fig. 5*E*), without any significant effects on s.c. tumor growth (Fig. S3*C*). Thus, stable suppression of PHIP in human melanoma cells suppressed the invasive and metastatic phenotypes observed in the murine model.

We then determined whether the genes and pathways affected after targeted suppression of PHIP are involved in mediating its effects on human melanoma invasion. Overexpression of human *TLN1* into C8161.9 cells stably expressing anti-*PHIP* shRNA (Fig. S3 *D* and *E*) resulted in significantly increased invasion into matrigel (Fig. 5*F*). In addition, transfection of a plasmid encoding *AKT2*, an AKT isoform implicated in tumor invasion and metastasis (16, 17), in C8161.9 cells stably expressing anti-*PHIP* shRNA, significantly increased their invasive capacity (Fig. 5*G*). Thus, the proinvasive role of PHIP is mediated, at least in part, by activating TLN1 and AKT.

Finally, we examined the impact of regulation of PHIP expression in the remaining cell lines in our panel. Overexpression of shRNA127738 into LOX cells resulted in significantly reduced invasion into matrigel (Fig. 4*F*). By contrast, overexpression of the human *PHIP* cDNA (Fig. S3*F*) resulted in significantly increased invasiveness of 1205Lu and D05 cells (Fig. 4 *G* and *H*).

Discussion

These results assign previously unreported tumor-promoting function to PHIP. Although PHIP has been shown to transduce signals downstream of IGF1R, its role in cancer has not been demonstrated. Here, we show that PHIP overexpression is both a marker that predicts and a mediator that promotes distant metastasis, the lethal event in melanoma progression. PHIP overexpression was an independent predictor of the development of both distant metastasis and death in human melanoma patients. These prognostic analyses confirm the direct relationship observed between PHIP overexpression and reduced survival in tumor-bearing mice. In addition, a large proportion of melanomas expressing high levels of PHIP harbored increased *PHIP* copy number. These results establish *PHIP*'s role both as a tumor progression marker and as a molecular mediator selected for during melanoma tumorigenesis.

Our results indicate that PHIP drives progression of melanoma in significant part through its regulation of pathways mediating tumor invasion. This observation is supported by recent studies demonstrating similar effects on tumor cell invasion and metastasis by using an anti-IGF1R antibody (18). In addition, microarray analysis revealed down-regulation of *Tln1* in melanoma cells with reduced *Phip* expression. TLN1, which is involved in the assembly of actin filaments, has been shown to mediate tumor invasion and metastasis through AKT-dependent effects (8). Furthermore, AKT itself plays an important role in melanoma progression (19–21). Thus, our results are consistent with a model

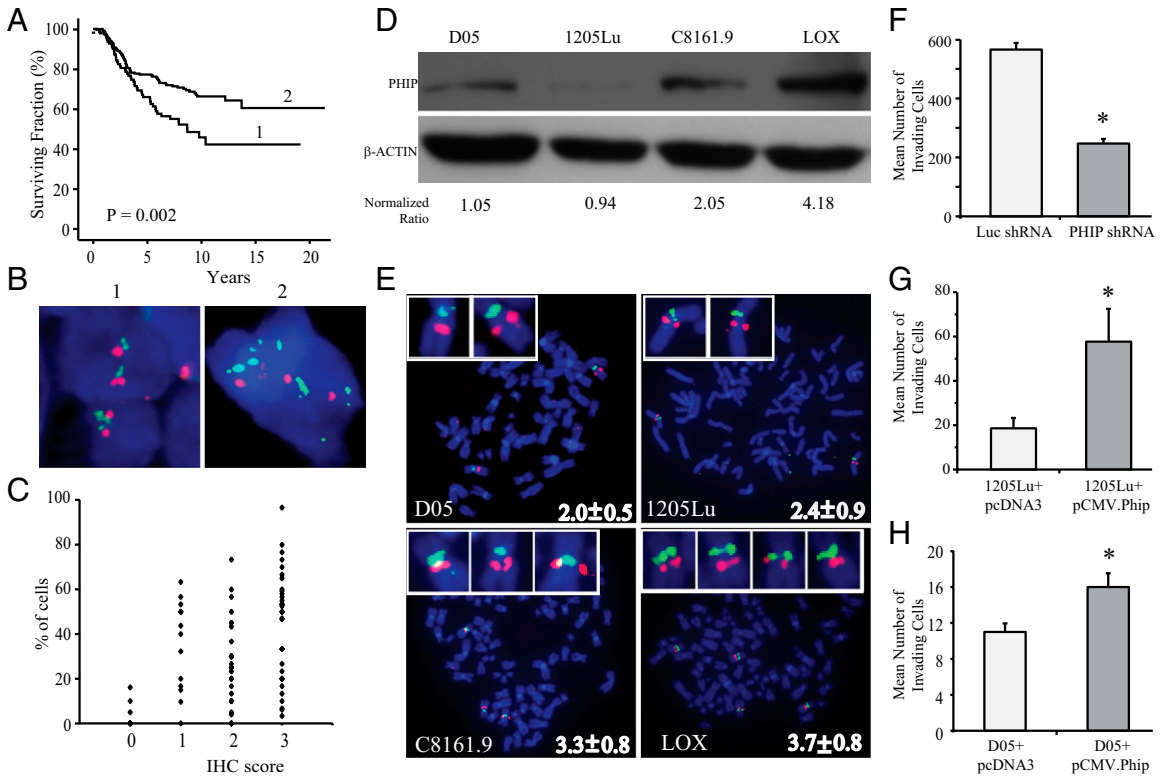

Fig. 4. Examination of PHIP levels in human melanoma tissues and cell lines. (*A*) Kaplan–Meier analysis of DSS in patients with highest PHIP expression levels (score of 3, curve 1) versus all other patients (score of 0–2, curve 2). (*B*) A composite image of nuclear counterstain and FISH signals from a pool of four BAC clones spanning the *PHIP* locus (red) and clones for 6p11.1 and 6q11.1 (green) from melanomas expressing the lowest (score of 0, *Left*) and highest (score of 3, *Right*) levels of PHIP protein expression. (*C*) Dot plot presenting the significant correlation between the immunohistochemical score and the percentage of cells with three or more copies of the *PHIP* locus in primary melanoma ($P < 0.001$). (*D*) Western blot analysis of PHIP expression in a panel of human melanoma cell lines and corresponding normalized ratio. (*E*) Representative FISH signals for the *PHIP* locus (red) and clones for 6p11.1 and 6q11.1 (green) in a panel of human melanoma cell lines. *Insets* represent enlarged chromosome 6 and corresponding *PHIP* copy number as mean and SD of number of signals. (*F*) Invasive capacity of LOX melanoma cells was reduced by 56% after overexpression of anti-*PHIP* shRNA compared with anti-luc shRNA. (*G*) Invasive capacity of 1205Lu cells was increased threefold after overexpression of *PHIP* cDNA compared with vector only. (*H*) Invasive capacity of D05 cells was increased 1.5-fold after overexpression of *PHIP* cDNA or vector only. *$P < 0.001$ versus control.

in which PHIP directs a coordinated program of melanoma cell invasion through the activation of TLN1 and AKT.

In addition, gene expression profiles of the NCI60 panel of cancer cell lines showed high levels of *PHIP* expression in melanoma and other solid tumors, including breast cancer and nonsmall cell lung cancer (22). Thus, PHIP may represent a rational therapeutic target against a range of different, lethal solid tumor types. The significant prolongation of survival produced by shRNA-mediated suppression of PHIP in tumor-bearing mice establishes the therapeutic relevance of PHIP targeting preclinically. However, additional studies will be required to assess how powerful a therapeutic approach PHIP inhibition is in the therapy of melanoma metastasis.

In the era of targeted therapy, solid tumors are characterized by overexpression or mutation of genes that play important roles in tumor progression. A high proportion of melanomas are characterized by BRAF, NRAS, or PTEN mutations. However, the molecular basis of triple-negative melanomas lacking these mutations is poorly characterized. Our results suggest that PHIP levels may be used to classify some melanomas that lack these three mutations. It is likely that additional molecular aberrations will be identified to further characterize triple-negative melanomas. Along with recent studies demonstrating that the IGF axis is activated in melanomas with acquired resistance to BRAF inhibition (23), these studies have identified IGF signaling as an important alternative pathway to promote melanoma progression. Overall, our studies identify PHIP as a molecular mediator of melanoma progression that also appears to function in the setting of a subset of triple-negative melanomas.

Materials and Methods

Additional technical details are provided in *SI Materials and Methods*.

Cell Culture. B16-F10 murine melanoma cells (ATCC), LOX human melanoma cells (kindly provided by O. Fodstad, Oslo University Hospital, Oslo, Norway), and D05 (kindly provided by B. Bastian, University of California, San Francisco, CA) were cultured in RPMI medium 1640 containing 5% (vol/vol) FBS. 1205Lu cells (kindly provided by B. Bastian) were cultured in MCDB153/Leibovitz medium (at 4:5) containing 2% (vol/vol) FBS and 1 μg/mL insulin. The highly metastatic C8161.9 human melanoma cells (24) (obtained from D. Welch, University of Alabama, Birmingham, AL) were grown in DMEM/Ham's F-12 (at 1:1) medium containing 10% (vol/vol) FBS and nonessential amino acids. All cells contained pen/strep in their respective media (University of California, San Francisco cell culture facility) and were passaged every 2–3 d (37 °C and 5% CO_2). For in vivo experiments, the cells were cultured up to the time of tail-vein injection when they were resuspended either in RPMI medium 1640 alone or DMEM/Ham's F-12 only.

Quantitative Real-Time PCR (qRT-PCR) Analysis. Total cellular RNA was extracted by using the RNeasy Mini Kit (Qiagen). For qRT-PCR (TaqMan assay; Applied Biosystems), cDNA was synthesized from 1 μg of total cellular RNA by using iScript cDNA Synthesis kit (BioRad Laboratories). Five microliters of cDNA was amplified by using final concentrations of 500 nM (each) forward and reverse primers, 200 nM probe (Applied Biosystems), 200 nM (each) dNTPs (Invitrogen), 1× buffer A (Applied Biosystems), and 0.025 unit/μL AmpliTaq Gold DNA Polymerase (Applied Biosystems). The amplification

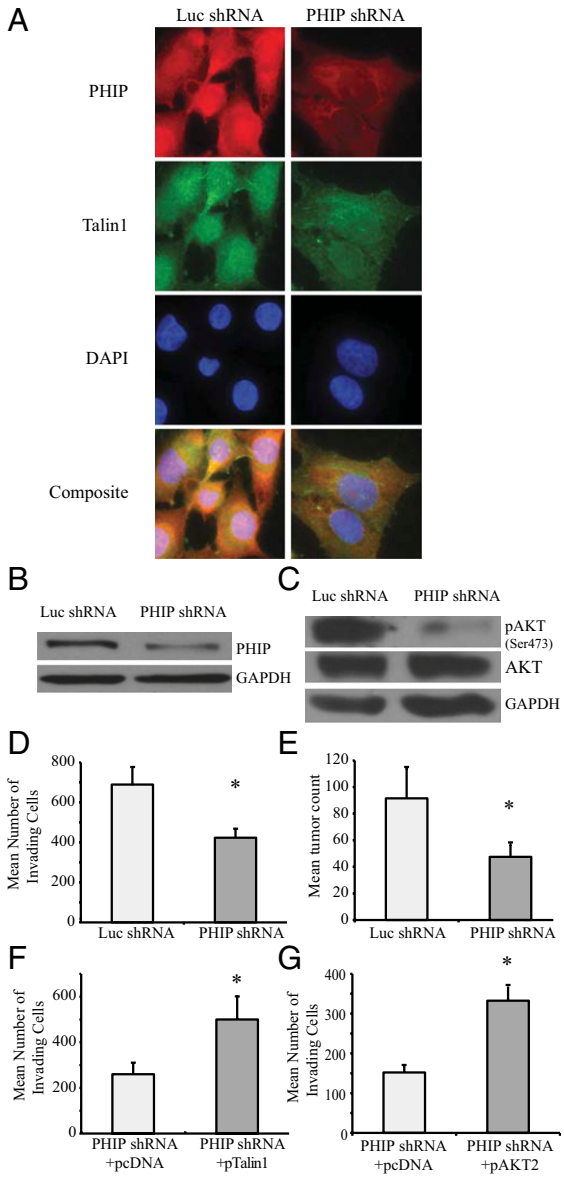

Fig. 5. Effects of modulation of PHIP expression in human melanoma cells. (*A*) Images representing immunofluorescent detection of PHIP and TLN1 in C8161.9 stable transformants expressing anti-luc shRNA or anti-*PHIP* shRNA. DAPI staining was used to counterstain the nuclei. (*B*) Western blot analysis of PHIP and GAPDH in C8161.9 stable transformants expressing anti-luc shRNA or anti-*PHIP* shRNA. (*C*) Western blot analysis of AKT and GAPDH, showing 86% reduction of pAKT levels in C8161.9 transformants expressing anti-*PHIP* shRNA-expressing cells compared with control cells expressing anti-luc shRNA, after normalization to GAPDH levels. (*D*) Invasion into matrigel was reduced by 38.5% in C8161.9 stable transformants expressing anti-*PHIP* shRNA compared with anti-luc shRNA. (*E*) Total tumor counts in the lungs of nude mice i.v. injected with C8161.9 stable transformants expressing anti-*PHIP* shRNA was reduced by 48% compared with those expressing anti-luc shRNA. (*F*) Overexpression of *TLN1* cDNA increased by twofold the invasive capacity of C8161.9 cells expressing anti-*PHIP* shRNA. (*G*) Transfection of *AKT2* cDNA increased by 2.2-fold the invasive capacity of C8161.9 stable transformants expressing anti-*PHIP* shRNA. $*P < 0.05$ versus control.

was conducted at 95 °C for 12 min and 45 cycles of 95 °C for 15 s and 60 °C for 1 min.

Invasion Assay. The Matrigel assay for tumor invasion was performed as described (25). For the B16-F10 and LOX cells, insert chambers were coated with 15 μL of matrigel at 6 mg/mL protein; 17 μL and 7 mg/mL for C8161.9 cells; 15 μL and 5 mg/mL for 1205Lu; and 15 μL and 4 mg/mL for D05 cells.

Tissue Arrays and Immunostaining. All biomarker analyses conducted herein on human specimens were approved by the Institutional Review Board. Tissue microarrays were created as described by using core diameters of 1.0 mm taken from the paraffin blocks (26, 27). Slides were prepared from formalin-fixed tissue microarrays and stained with anti-human PHIP monoclonal antibody at a 1:100 dilution (Abnova). Microwave antigen retrieval was conducted in 10 mM citrate buffer at pH 6.0. Endogenous peroxidase was blocked with 3% H_2O_2, and additional blocking was performed with normal rabbit serum. The primary antibody was diluted in 1.0% BSA in PBS and applied overnight at 4 °C. Antibody staining was observed by using biotin-labeled anti-goat IgG and avidin–biotin (Vector Laboratories) followed by diaminobenzidine. Sections were counterstained with hematoxylin.

Evaluation of Immunohistochemical Staining. The regions of most uniform staining were scored for each specimen, and the expression of PHIP protein was graded on cellular intensity by using the following scale: no staining (0), weak staining (1), moderate staining (2), and intense staining (3). The tissue microarrays and positive and negative control sections were scored by the study dermatopathologist (R.W.S.) twice, and a third consensus score was determined for any discrepant scoring. Statistical methods used to assess the significance of various prognostic factors on melanoma outcome were described (9). In all of the analyses shown, the cutpoint used for PHIP expression included cases with the highest PHIP expression levels (score of 3) versus all other cases (score of 0–2).

Western Blotting. B16-F10 and C8161.9 stable transformants were starved for 4 h in RPMI medium 1640 or DMEM/Ham's F-12 (at 1:1) medium only, respectively, and stimulated with 5 μg/mL insulin for 5 min before protein extraction was carried out from adherent cells according to the manufacturer's protocol (Santa Cruz Biotechnology). Fifty micrograms of protein was electrophoresed in 10% Tris·HCl denaturing gels (Bio-Rad) and transferred onto nitrocellulose membranes (Bio-Rad). Membranes were first incubated overnight at 4 °C with each antibody and then with their respective horseradish peroxidase-labeled secondary antibodies for 1 h at room temperature: goat anti-mouse HRP (no. 12–349 at 1:1,000 dilution; Millipore) and bovine anti-rabbit HRP (no. sc-2370 at 1:1,000 dilution; Santa Cruz Biotechnology). Binding was detected by using luminol reagent (Santa Cruz Biotechnology). For PHIP protein detection in C8161.9 and B16-F10 clones, 50 μg of protein was electrophoresed in 5% Tris·HCl denaturing gels (Bio-Rad) and membranes were first incubated overnight at 4 °C with the anti-human PHIP monoclonal antibody (1:100 dilution; Abnova). The anti-mouse HRP (no. 12–349 at 1:1,000 dilution; Millipore) was incubated for 1 h at room temperature as a secondary antibody.

Gene Expression Profiling. cDNA microarray analysis was performed as described (7).

Genotyping. Genomic DNA was extracted from formalin-fixed paraffin-embedded (FFPE) tissues. Briefly, FFPE tissues were scraped from 10 slides (5 μm) and deparaffinized with xylene followed by a wash with 100% ethanol. Then, DNA was extracted by using the QIAmp DNA kit (Qiagen).

The genomic sequence of *PTEN* (GenBank accession no. NM_000314) was used to design a set of primers and probe specific to the *PTEN* gene exon 5 (Primer Express software version 1.0; Applied Biosystems). The primers and probe for RNase P used as an endogenous control gene were obtained from Applied Biosystems. The RNase P probe was labeled at 5′ end with VIC (Applied Biosystems) instead of FAM. *PTEN* copy number was determined by relative quantification using the ΔΔCt method normalized to the RNase P copy number of 2^{20}. To analyze the results from the copy number experiment, we used the TaqMan Gene Copy Number Assays Macro File (Applied Biosystems). The presence of *NRAS Q61R* or *BRAF V600E* mutations was confirmed by sequencing after performing a PCR amplification with the primer sets targeting each codon. The amplification of genomic DNA was conducted at 95 °C for 5 min and 10 cycles of 95 °C for 30 s, 65 °C for 90 s, 72 °C for 90 s followed by 32 cycles of 95 °C for 30 s, 57 °C for 60 s, and 72 °C for 60 s.

FISH and Microscopy. BAC clones RP11-767O1, RP11-484L10, RP11-217L13, and CTD-2297E14 were used to detect the *PHIP* locus and clones RP11-26M18 and RP11-136K2 were used to detect 6q11.1 and 6p11.1, respectively (February 2009 freeze of the University of California, Santa Cruz Genome Browser, http://genome.ucsc.edu). All clones were obtained from the Children's Hospital of Oakland Research Institute (CHORI). BAC DNAs were prepared with the Large-Construct kit (Qiagen) and labeled by nick translation with Alexa Fluor 488 and 594 dUTPs (Molecular Probes) as described (28). The quality and mapping of all probes were verified by hybridization to normal metaphase spreads in combination with a commercially available centromeric probe for

chromosome 6 (Openbiosystems), before cell line and tissue analysis. Hybridization on cell lines and tissue microarrays was performed as described (28, 29). Images were taken with a Zeiss Axio Imager Z2 controlled by Axiovision software.

Analysis of FISH Results. The FISH signals were assessed and counted manually from images with several Z stack layers acquired by using Zeiss Axio Image Z2 microscope controlled by AxioVision software. A minimum of 20 nuclei from each case and cell line were evaluated, and the signals were interpreted according to guidelines described (30) and were recorded as 1 through 5 signals or greater. FISH signals from BAC clones for 6q11.1 and 6p11.1 were interpreted as the centromeric signal, and a ratio was calculated by dividing the number of PHIP signals by the number of centromeric signals for each cell and reported as mean and SD for each case. The FISH signals for the PHIP locus in melanomas with an immunohistochemical score of 0 for PHIP were used to determine a cutoff value (mean + 2× SD) for percent cells with three or more signals (18.5%, interpreted as 20%). This cutoff was then uniformly applied in all statistical analyses.

Immunofluorescence. Quantification of PHIP and TLN1 expression using immunofluorescence was performed on cells cultured on coverslips as described (31). The anti-PHIP (1:250 dilution) and anti-TLN1 (no. ab71333 at 1:500 dilution; Abcam) antibodies were detected by using secondary antibodies labeled with Alexa Fluor 594 or Alexa Fluor 488, respectively (both at 1:1,000 dilution; Molecular Probes). Images were taken at fixed exposures with a Zeiss Axio Image Z2 microscope, and the fluorescence intensities of individual cells were quantified by using ImageJ software. The mean pixel intensities were used for statistical analysis using Microsoft Excel and Data Desk.

Animal Studies. All animal care was in accordance with institutional guidelines and a protocol that was approved by the University of California San Francisco Committee on Animal Research. Groups of 45-d-old female C57BL/6 (Charles River) were inoculated by tail vein injection with 30,000 B16-F10 cells. In the therapeutic study, two i.v. injections of cationic liposome DNA complexes (CLDCs) containing plasmid DNA expressing various shRNA constructs were performed at days 3 and 10 after tumor cell inoculation as described (27). Groups of 10 45-d-old female nude mice (Charles River) were injected i.v. with 100,000 C8161.9pLKO1 stably transfected cells. The number of metastatic lung tumors was counted.

Statistical Methods. All quantified data represents an average of at least triplicate samples or as indicated. Error bars represent standard error of the mean. Statistical significance was determined by the Student *t* test, Mann–Whitney test, or Kolmogorov–Smirnov test, and P values <0.05 were considered significant. The correlation between *PHIP* copy number and immunohistochemical score was tested by regression analysis using Data Desk software.

ACKNOWLEDGMENTS. We thank the Helen Diller Family Comprehensive Cancer Center Preclinical, Genome Analysis, and Tissue Core Facilities for the assistance with animal studies, quantitative RT-PCR designs, and immunostaining, respectively; Swapna Vemula for assistance in the detection of *BRAF* and *NRAS* mutations; and Allan Balmain and David Stokoe for review of the manuscript. This work was supported by the Mary R. and Joseph R. Payden Foundation, the Herschel and Diana Zackheim Endowment Fund, and National Institutes of Health Grants CA114337, CA122947 (to M.K.-S.), and CA109171 (to R.J.D.).

1. Chapman PB, et al.; BRIM-3 Study Group (2011) Improved survival with vemurafenib in melanoma with BRAF V600E mutation. *N Engl J Med* 364:2507–2516.
2. Baserga R (2009) Customizing the targeting of IGF-1 receptor. *Future Oncol* 5:43–50.
3. Hofmann F, García-Echeverría C (2005) Blocking the insulin-like growth factor-I receptor as a strategy for targeting cancer. *Drug Discov Today* 10:1041–1047.
4. Manning BD, Cantley LC (2007) AKT/PKB signaling: Navigating downstream. *Cell* 129: 1261–1274.
5. Podcheko A, et al. (2007) Identification of a WD40 repeat-containing isoform of PHIP as a novel regulator of beta-cell growth and survival. *Mol Cell Biol* 27:6484–6496.
6. Li S, et al. (2010) The full-length isoform of the mouse pleckstrin homology domain-interacting protein (PHIP) is required for postnatal growth. *FEBS Lett* 584:4121–4127.
7. Haqq C, et al. (2005) The gene expression signatures of melanoma progression. *Proc Natl Acad Sci USA* 102:6092–6097.
8. Sakamoto S, McCann RO, Dhir R, Kyprianou N (2010) Talin1 promotes tumor invasion and metastasis via focal adhesion signaling and anoikis resistance. *Cancer Res* 70: 1885–1895.
9. Rangel J, et al. (2006) Prognostic significance of nuclear receptor coactivator-3 overexpression in primary cutaneous melanoma. *J Clin Oncol* 24:4565–4569.
10. Balch CM, et al. (2009) Final version of 2009 AJCC melanoma staging and classification. *J Clin Oncol* 27:6199–6206.
11. Bauer J, Bastian BC (2006) Distinguishing melanocytic nevi from melanoma by DNA copy number changes: Comparative genomic hybridization as a research and diagnostic tool. *Dermatol Ther* 19:40–49.
12. Blokx WA, van Dijk MC, Ruiter DJ (2010) Molecular cytogenetics of cutaneous melanocytic lesions - diagnostic, prognostic and therapeutic aspects. *Histopathology* 56: 121–132.
13. Dankort D, et al. (2009) Braf(V600E) cooperates with Pten loss to induce metastatic melanoma. *Nat Genet* 41:544–552.
14. Tsao H, Goel V, Wu H, Yang G, Haluska FG (2004) Genetic interaction between NRAS and BRAF mutations and PTEN/MMAC1 inactivation in melanoma. *J Invest Dermatol* 122:337–341.
15. Damsky WE, et al. (2011) β-catenin signaling controls metastasis in Braf-activated Pten-deficient melanomas. *Cancer Cell* 20:741–754.
16. Dillon RL, Muller WJ (2010) Distinct biological roles for the akt family in mammary tumor progression. *Cancer Res* 70:4260–4264.
17. Arboleda MJ, et al. (2003) Overexpression of AKT2/protein kinase Bbeta leads to up-regulation of beta1 integrins, increased invasion, and metastasis of human breast and ovarian cancer cells. *Cancer Res* 63:196–206.
18. Sachdev D, Zhang X, Matise I, Gaillard-Kelly M, Yee D (2010) The type I insulin-like growth factor receptor regulates cancer metastasis independently of primary tumor growth by promoting invasion and survival. *Oncogene* 29:251–262.
19. Govindarajan B, et al. (2007) Overexpression of Akt converts radial growth melanoma to vertical growth melanoma. *J Clin Invest* 117:719–729.
20. Meier F, et al. (2005) The RAS/RAF/MEK/ERK and PI3K/AKT signaling pathways present molecular targets for the effective treatment of advanced melanoma. *Front Biosci* 10: 2986–3001.
21. Ramaswamy S, et al. (1999) Regulation of G1 progression by the PTEN tumor suppressor protein is linked to inhibition of the phosphatidylinositol 3-kinase/Akt pathway. *Proc Natl Acad Sci USA* 96:2110–2115.
22. Ross DT, et al. (2000) Systematic variation in gene expression patterns in human cancer cell lines. *Nat Genet* 24:227–235.
23. Villanueva J, et al. (2010) Acquired resistance to BRAF inhibitors mediated by a RAF kinase switch in melanoma can be overcome by cotargeting MEK and IGF-1R/PI3K. *Cancer Cell* 18:683–695.
24. Miele ME, et al. (2000) A human melanoma metastasis-suppressor locus maps to 6q16.3-q23. *Int J Cancer* 86:524–528.
25. Kashani-Sabet M, et al. (2002) Identification of gene function and functional pathways by systemic plasmid-based ribozyme targeting in adult mice. *Proc Natl Acad Sci USA* 99:3878–3883.
26. Kononen J, et al. (1998) Tissue microarrays for high-throughput molecular profiling of tumor specimens. *Nat Med* 4:844–847.
27. Kashani-Sabet M, et al. (2004) NF-kappa B in the vascular progression of melanoma. *J Clin Oncol* 22:617–623.
28. Wiegant J, Raap AK (2001) Probe labeling and fluorescence in situ hybridization. *Curr Protoc Cytom* 8:8.3.
29. Chin SF, et al. (2003) A simple and reliable pretreatment protocol facilitates fluorescent in situ hybridisation on tissue microarrays of paraffin wax embedded tumour samples. *Mol Pathol* 56:275–279.
30. Munné S, Márquez C, Magli C, Morton P, Morrison L (1998) Scoring criteria for preimplantation genetic diagnosis of numerical abnormalities for chromosomes X, Y, 13, 16, 18 and 21. *Mol Hum Reprod* 4:863–870.
31. Van Raamsdonk CD, et al. (2009) Frequent somatic mutations of GNAQ in uveal melanoma and blue naevi. *Nature* 457:599–602.